

GOBINA, E., SHEHU, H. and ORAKWE, I. 2021. Predicting multicomponent gas transport in hybrid inorganic membranes. In *Proceedings of the ICANM 2021: 8th International conference and exhibition on advanced and nanomaterials 2021 (ICANM 2021)*, 9-11 August 2021, [virtual conference]. Ontario: ICANM, pages 47-56.

# Predicting multicomponent gas transport in hybrid inorganic membranes.

GOBINA, E., SHEHU, H. and ORAKWE, I.

2021

# Predicting Multicomponent Gas Transport In Hybrid Inorganic Membranes

\**Edward Gobina<sup>1</sup>, Habiba Shehu and Ifeyinwa Orakwe*

Robert Gordon University, Sir Ian Wood Building, Garthdee Road, Aberdeen, AB10 7GJ, United Kingdom.

\*Corresponding Author (email: [e.gobina@rgu.ac.uk](mailto:e.gobina@rgu.ac.uk); tel: +441224262348)

**Abstract-** A repeated dip-coating technique has been used to prepare novel inorganic multilayered membranes. The membranes have been characterized by Scanning Electron Microscopy (SEM) and nitrogen adsorption (ASAP 2010) respectively. The three-parameter model incorporating the gas transport characteristics of the hybrid membranes has been adequately described using a combination of Knudsen and Viscous flows. The model has been used to predict gas transport rates through the membranes over a wide range of gas compositions and good agreement has been observed with experimental data. The model has also been applied to estimate the separation layer thickness. The estimated value of 1.6 $\mu$ m is in good agreement with that of 1.62 $\mu$ m observed by scanning electron microscopy. The gases studied include O<sub>2</sub>, N<sub>2</sub>, He, H<sub>2</sub> and mixtures of CO<sub>2</sub>/N<sub>2</sub> and O<sub>2</sub>/N<sub>2</sub>, respectively. All experiments were carried out at room temperature and were found to possess both Knudsen and viscous flow as predicted by the model

**Index Terms:** Hydrogen, Alumina, Membranes, Dip-coating, Permeance.

**Introduction:** Membrane technology for gas separation and production processes is becoming an important and enabling technology in the current global decarbonisation efforts aimed at combating climate change and ensuring energy security. It is still ‘work in progress’ before H<sub>2</sub> is fully adopted as the global energy carrier to replace fossil fuels. During this transition period from fossil fuels to low-carbon sources, research into several gas separation and purification processes is gaining increased attention. One of these processes is membrane technology which offers several advantages in carbon capture, oxygen separation and hydrogen. Membranes processes are more energy efficient, cost effective and modular with the prospect of being widely deployable in offshore abandoned facilities such as oil and gas platforms and subsea infrastructure. Alumina membranes are thermally and chemically stable and can withstand harsh operating conditions.

**Experimental:** The experiment was carried out for a macroporous  $\alpha$ -alumina support with a 30 nm pore size and i.d= 7mm, o.d= 10 mm, effective length= 0.34 m. Another 30 nm  $\alpha$ -alumina support was graded with AlOOH sol and converted to  $\gamma$ -alumina by 5 sequential dippings using the dip coating method. The objective was to investigate the hydrogen permeation and selectivity at high temperature including the gas transport mechanisms. The tubes were dried at 65 °C for 2 hours in an oven to remove any water vapor or moisture and sealed at both ends. The modification of the  $\alpha$ -Al<sub>2</sub>O<sub>3</sub> support was carried out through a multilayer deposition process using a dipping-drying-calcining method. After each dipping, the support was dried for 10 hours at 65 °C and calcined at 873

K for 24 hours. Permeation tests were carried out in a membrane reactor module at 298, 323, 373, 473 and 573K.

**Theoretical Considerations:** The permeance,  $F_0$  of a gas through the multilayered inorganic membrane is the gas flux,  $Q$  (i.e., the gas flowrate, of divided by the membrane area, A) divided by the pressure drop,  $P_1$ - $P_2$  across the membrane. In the simplest approximation the permeance is the sum of a Viscous and Knudsen contribution and can be described by equation 1:

$$F_0 = F_{Knudsen} + F_{Viscous} \left( \frac{mol}{m^2 s} \right) \quad (1)$$

where  $F_{Knudsen}$  and  $F_{Viscous}$  are the Knudsen and viscous contributions respectively and are defined by:

$$F_{Knudsen} = \frac{8r_p(P_1 - P_2)}{3\delta(2\pi MRT)^{\frac{1}{2}}} \left( \frac{mol}{m^2 s} \right) \quad (2)$$

$$F_{Viscous} = \frac{r_p^2(P_1^2 - P_2^2)}{16\delta\mu RT} \left( \frac{mol}{m^2 s} \right) \quad (3)$$

Substituting equations (2) and (3) into equation (1) gives equation 4:

$$F_0 = \frac{8r_p(P_1 - P_2)}{3\delta(2\pi MRT)^{\frac{1}{2}}} + \frac{r_p^2(P_1^2 - P_2^2)}{16\delta\mu RT} \quad (4)$$

Equation (4) can be normalized to take into consideration the separating layer thickness. This is achieved by multiplying both the L.H.S. and R.H.S.

of equation 4 by  $\frac{\delta}{(P_1 - P_2)}$  to give equation (5):

$$\frac{F_0\delta}{(P_1 - P_2)} = F_T = \frac{8r_p}{3(2\pi MRT)^{\frac{1}{2}}} + \frac{r_p^2(P_1 + P_2)}{16\mu RT} \left( \frac{molm}{m^2 sPa} \right) \quad (5)$$

where  $F_T$  is the normalized permeance or permeability of the multilayered membrane.

Equation (5) can also be written in the more convenient form of equation 6:

$$F_T = \frac{8r_p}{3(2\pi MRT)^{1/2}} + \frac{r_p^2}{8\mu RT} \left( \frac{P_1 + P_2}{2} \right) \left( \frac{molm}{m^2 sPa} \right) \quad (6)$$

Equation (6) can be written in a more compact form as:

$$F_T = K_0 + B_0 P_{Average} \quad (7)$$

where:

$$K_0 = \frac{8r_p}{3(2\pi MRT)^{1/2}} \left( \frac{molm}{m^2 sPa} \right), \quad B_0 = \frac{r_p^2}{8\mu RT} \left( \frac{molm}{m^2 sPa^2} \right), \quad \text{and}$$

$$P_{Average} = \left( \frac{P_1 + P_2}{2} \right) (Pa)$$

Equation (7) is straight line of  $F_T$  is plotted against  $P_{Average}$  resulting in a slope equal to  $B_0$  and an intercept on the  $F_T$  axis equal to  $K_0$ . The nature of the straight line will indicate the extent of the  $F_T$  relative contributions of Viscous and Knudsen flow.

If the graph plotted is of the form  $F_T = B_0 P_{Average}$  then the flow is characterised by viscous flow. If, however, the graph plotted is of the form  $F_T = B_0 P_{Average} + K_0$ , then both the Knudsen flow and viscous flow contribute to the transport characteristics. Analysis of the intercept and the slope will then yield the values of an  $K_0$  and  $B_0$ , which upon substitution into equation (6) will enable estimation of the pore radius of the multilayered membrane.

Examination of equations (2) and (3) shows that several possibilities exist.

(i) For Knudsen flow:

$$\frac{F_{0,A}}{F_{0,B}} = \sqrt{\frac{M_B}{M_A}} \quad (8)$$

(ii) For Viscous flow:

$$\frac{F_{0,A}}{F_{0,B}} = \frac{\mu_B}{\mu_A} \quad (9)$$

The mean free path of a gas molecule is given by equation (10):

$$\lambda = 2r_p \cdot \text{Knudsen Coefficient (m)} \quad (10)$$

In the equation (7), both  $B_0$  and  $K_0$  depend on the membrane material characteristics such as thickness of the separating layer, the porosity, tortuosity, and

pore radius. Temperature and type of gas also influence  $B_0$  and  $K_0$  as described by equation (11):

$$B_0 \sim 1/\mu T \quad \text{and} \quad K_0 \sim 1/MT \quad (11)$$

where  $\mu$  is the viscosity,  $T$  the temperature and  $M$  the gas molecular weight. Viscosities of most gases are relatively close to each other and therefore it is obvious that the gas separation will mainly depend on the difference in the molecular weight, and this will be determined by the Knudsen flow contribution of equation (6) as shown in equation (8) for a gas mixture containing components A and B.

Equation (7) is only a simple approximation where the pressure difference is the driving force for gas transport through the multilayered membrane and does not consider other transport mechanism such as surface flow, multilayer diffusion, capillary condensation, and molecular sieving. It however gives a good indication of the performance and quality of the membrane provided that the necessary precautions are achieved to before and during gas transport measurements.

**Results and Discussion:** PLATE 1 shows a SEM x-sectional and top view of the hybrid membrane. It reveals a dense film formed on the outside surface of the support tube. Using SEM, it is possible to estimate that the thickness of this layer is  $1.62 \times 10^{-6}m$ , which agrees with the calculated value of  $1.6 \times 10^{-6}m$ , obtained from the method of resistance combination.

Gas permeation experiments of hybrid inorganic membrane are carried out to check the quality and evaluate the transport mechanism/pore size. High quality hybrid inorganic membranes (free of macro defects) usually show a non-dependence of permeability as a function of average transmembrane pressure. Figure 1 shows the permeability of pure and mixed-gas through the hybrid inorganic membrane. The permeability shows a slight dependence in the average transmembrane pressure. The evidence of a small but noticeable viscous flow contribution demonstrates that the hybrid inorganic membrane contains a small number of defects. The macrodefect, might have been generated during the drying period or due to incompatibility between the support and the sol.

Table 1 shows the experimental pore radius calculated for the various gases using the three-parameter model for the hybrid inorganic membrane. The values agree with Knudsen selectivity and data found in the literature for different hybrid types including zeolites and MOR (mordenite). The measured permeance permeability values

are typically in the range of those reported in the literature for zeolitic membrane systems [4].

Linear regression has been used to obtain the Knudsen and viscous flow constants  $K_0$  and  $B_0$  of equation 7. Plots of these are presented in Figures 2, 3, 4 and 5 for pure gases oxygen, nitrogen, helium, and hydrogen respectively, showing good correlation of the experimental data with the three-parameter model. Values of  $K_0$  and  $B_0$  for oxygen and nitrogen were then used to predict the permeability of a mixed gas system. This is shown in Figures 6 and 7 which are a parity diagram. Here also, good agreement has been observed between the predicted permeability and the calculated permeability.

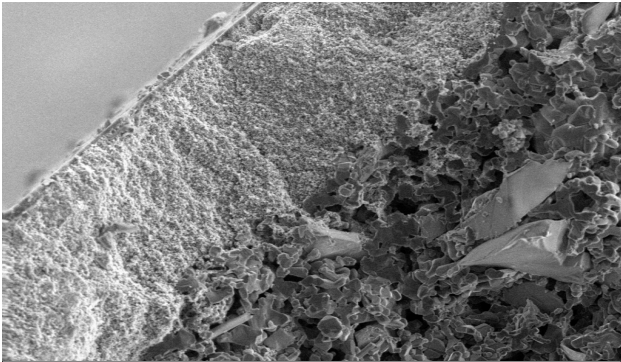


PLATE 1: SEM image of cross-sectional area of the macroporous  $\alpha$ -alumina support (resolution 1000 x)

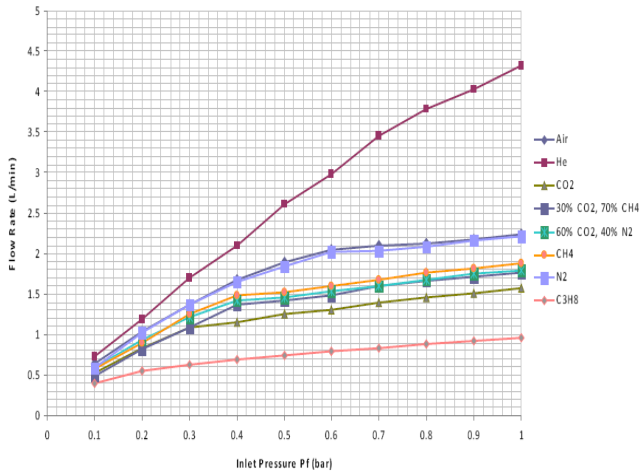


Figure 1. Pure and mixed gas flowrate against inlet pressure.

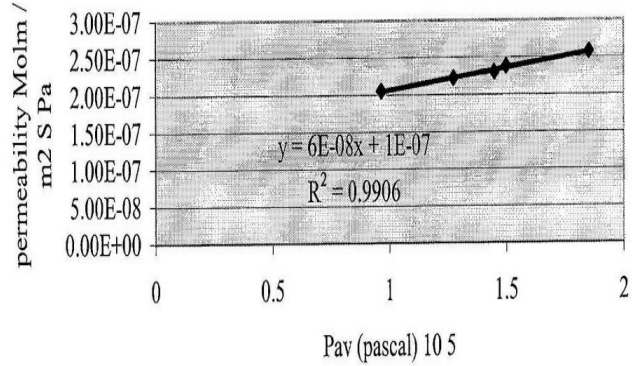


Figure 2. Permeability of oxygen at room temperature vs average transmembrane pressure.

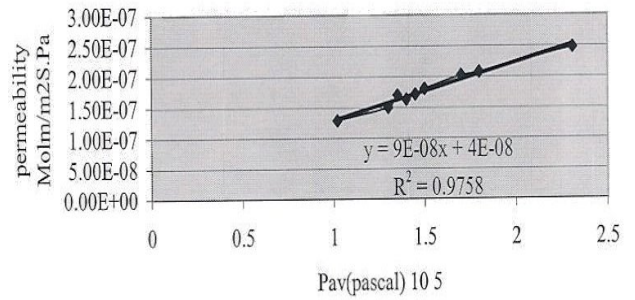


Figure 3: Permeability of nitrogen at room temperature vs average transmembrane pressure.

Table 1: Estimated pore sizes of the hybrid membrane in respect to  $K_0$  and  $B_0$ .

Gases	r estimated from $K_0$	r estimated from $B_0$
Hydrogen	$1.4 \times 10^{-7} \text{m}$	$7.07 \times 10^{-3} \text{m}$
Helium	$1.8 \times 10^{-7} \text{m}$	$1.244 \times 10^{-2} \text{m}$
Argon	$1.4 \times 10^{-4} \text{m}$	Null
Air	$5.03 \times 10^{-5} \text{m}$	$8.8 \times 10^{-2} \text{m}$
Nitrogen	$9.903 \times 10^{-6} \text{m}$	$5.446 \times 10^{-2} \text{m}$
Oxygen	$2.646 \times 10^{-5} \text{m}$	$2.76 \text{m}$

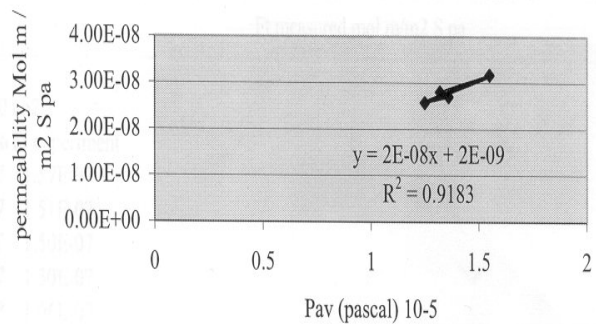


Figure 4: Permeability of helium at room temperature vs average transmembrane pressure.

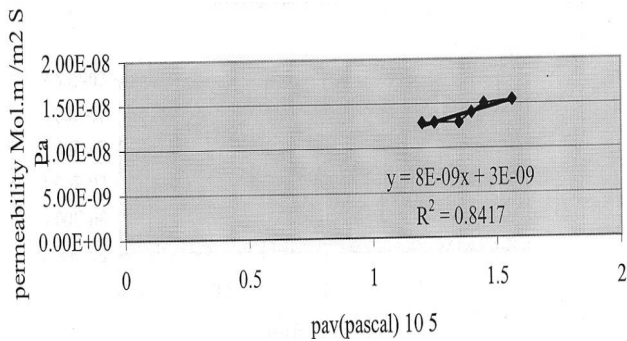


Figure 5: Permeability of hydrogen at room temperature vs average transmembrane pressure.

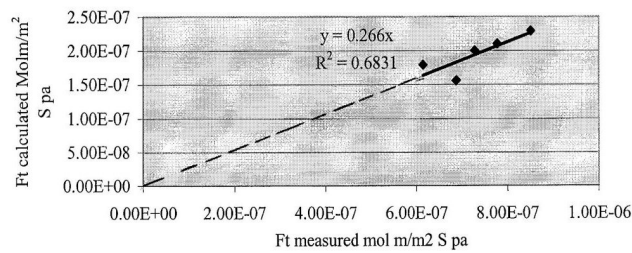


Figure 6: Parity diagram for calculated vs measured mixed gas permeability (40% O<sub>2</sub> / 60% N<sub>2</sub>)

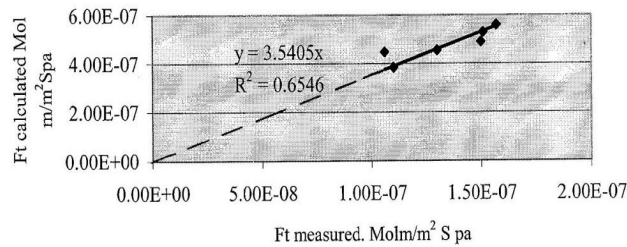


Figure 7: Parity diagram for calculated vs measured mixed gas permeability (20% O<sub>2</sub> / 80% CO<sub>2</sub>)

### Conclusion:

Gas diffusion properties of modified alumina ceramic membrane was investigated. Five gases CO<sub>2</sub>, H<sub>2</sub>, N<sub>2</sub>, He and Ar with mixtures were used for the permeation test. Overall results confirm that Membrane the gas flow rate of the single and gas mixtures can be predicted by Knudsen and viscous flow using the combination of resistance method. The single gas flow rate increases with an increase in pressure. A comprehensive permeability determination confirms that the modification process resulted in conformal coverage. The significance of Knudsen and viscous flow mechanisms were beneficial and gave a better understanding of their individual contribution on the hydrodynamics of the membrane and pore size prediction.

**Acknowledgement:** Sincere thanks to CCEMC (ERA) Canada and PTFDF, Nigeria for sponsorship of this work.

### References:

1. X. Li, B. Liang, Journal of the Taiwan Institute of Chemical Engineers, 43(2012) 339-346.
2. X. Changrong, W. Feng, M. Zhaojing, L. Fanqing, P. Dingkun, M. Guanyao, Journal of Membrane Science 116 (1996) 9-16.
3. Y. Wall, O. Aime-Mudimu, G. Braun, G. Brunner, Desalination 230 (2010) 1056-1059.
4. Yunfeng, G, S, T, Oyama, Journal of Membrane Science 306 (2007) 216-277.

### Nomenclature

T	Atmospheric temperature (K)
P <sub>1</sub>	Atmospheric pressure + gauge pressure (bar)
P <sub>2</sub>	Atmospheric pressure (bar)
P <sub>Average</sub>	Average pressure (bar) $\left[ \frac{P_1 + P_2}{2} \right]$
F <sub>0</sub>	Total gas flux through the membrane $\left( \frac{mol}{m^2 s} \right)$
F <sub>Viscous</sub>	Viscous flow gas flux through the membrane $\left( \frac{mol}{m^2 s} \right)$
F <sub>Knudsen</sub>	Knudsen flow gas flux through the membrane $\left( \frac{mol}{m^2 s} \right)$
F <sub>T</sub>	Permeability $\left( \frac{mol.m}{m^2 s Pa} \right)$
r <sub>p</sub>	Membrane pore size (m)
δ	Membrane wall thickness (m)
M	Molecular weight $\left( \frac{g}{mol} \right)$
R	Molar gas constant $\left( 8.3145 \left( \frac{kJ}{kgK} \right) \right)$
μ	Viscosity $\left( \frac{kg}{ms} \right)$
λ	Mean free path (m)